Monitoring the heat-induced structural changes of alkaline phosphatase by molecular modeling, fluorescence spectroscopy and inactivation kinetics investigations

**Loredana Dumitrașcu · Nicoleta Stănciuc ·
Iuliana Aprodu · Ana-Maria Ciuciu · Petru Alexe ·
Gabriela Elena Bahrim**

Abstract The heat induced conformational changes of calf alkaline phosphatase (ALP) were analyzed using different methods, based on fluorescence spectroscopy, molecular modeling and inactivation studies. Experimental studies were conducted in buffer solution in the temperature range between 25 and 70 °C. Molecular dynamic (MD) simulation provided details on thermally induced changes in ALP structure, highlighting that heating favored the hydrophobic exposure and important alteration of the catalytic site above 60 °C. Additional information to MD data were obtained by using different fluorescence spectroscopy methods, which revealed a complex mechanism of thermal denaturation. Therefore, the emissive properties indicated an unfolding of ALP at temperatures below 60 °C, whereas at higher temperatures, the polypeptides chains fold leading to a higher exposure of Trp residues. In order to establish a structure-function relationship, the results were correlated with inactivation studies of ALP in buffer at pH 9.0. The inactivation data were fitted using a first-order kinetic model, resulting in an activation energy value of 207.26 ± 21.68 kJ·mol^{-1}.

Keywords Alkaline phosphatase · Molecular modeling · Fluorescence spectroscopy · Inactivation kinetics

L. Dumitrașcu · N. Stănciuc (✉) · I. Aprodu · A.-M. Ciuciu ·
P. Alexe · G. E. Bahrim
Faculty of Food Science and Engineering, Dunarea de Jos University
of Galati, Domneasca Street 111, Building E, Room 304,
800201 Galati, Romania
e-mail: nsava@ugal.ro
URL: http://www.bioaliment.ugal.ro

Introduction

Alkaline phosphatase (ALP, EC 3.1.3.1) is an enzyme, commonly found in nature, in all organisms from bacteria to mammals. ALP of bacterial origin, frequently have higher thermal stability than ALP of bovine origin (Knight and Fryer 1989). ALP is considered one of the most versatile and widespread protein fold, and represents a typical example of tertiary structure adopted by various enzymes during divergent evolution (Hung and Chang 2001). Different isozymes of ALP are grouped under two categories: the tissue specific ALP and tissue non-specific ALP (Zalatan et al. 2008). ALP is a membrane bound glycoprotein having sialic acid as sugar moiety (Rankin et al. 2010), responsible for dephosphorylation of different compounds, such as nucleotides, proteins, and alkaloids under alkaline conditions. The enzyme takes the form of a dimer consisting of two identical subunits of molecular weight of 94 kDa. ALP is a metalloenzyme that contains three metal ions, two zinc ions per molecule in each catalytic site, necessary for the activation of the enzyme, and one magnesium ion that enhances the activity (Wang et al. 2014). Enzyme activity is inhibited by metal chelators such as Co^{2+}, Cu^{2+}, and Sn^{2+} (Fox and Kelly 2006). ALP has two intramolecular disulfide bonds per monomer, formed after export to the periplasmic space, with important functional roles, such as stabilization of the protein structure (Cys^{168}–Cys^{178}) and supporting the enzymatic activity (Cys^{286}–Cys^{336}) (Michio et al. 1997).

In dairy industry, ALP is widely used for assessing the efficiency of milk pasteurization (High Temperature Short Time) (Marchand et al. 2009), based on the fact that this enzyme presents a higher thermal resistance when compared with some pathogenic microorganisms. A negative test for ALP guarantees destroying most unsporulated pathogenic

bacteria potentially presented in milk, ensuring the consumer that the product can be consumed without having adverse health effects.

In addition, ALP is one of the most commonly assayed enzymes in clinical practice because the change of ALP level is connected with a variety of physiological diseases such as bone diseases, hepatitis, obstructive jaundice, breast and prostatic cancer, diabetes, etc. (Liu et al. 2014).

The present study was aimed to investigate the influence of heat treatment on conformational properties of the bovine (calf) intestine ALP (calf intestinal mucosa represents a rich source of intestinal ALP) based on fluorescence spectroscopy, inactivation kinetics and molecular modeling. The findings of our study may provide important insights in the dynamic denaturation process of ALP, which are expected to allow advanced understanding of the enzyme behavior in complex matrices, in qualitative or quantitative immunoassays, in development of bioanalytical assays based on the enzymatic generation of nanoparticles, etc.

Materials and methods

Materials

Commercial ALP (120.4 U·mg^{-1} lyophilized powder) was purchased from AppliChem GmbH (Ottoweg 4, Darmstadt, Germany), *p*-nitrophenyl phosphate liquid substrate system, acrylamide, potassium iodide (KI) and 1-anilinonaphthalene-8-sulfonic acid (ANS) were purchased from Sigma (Sigma-Aldrich Co, St. Louis, MO). The protein was used without further purification. All other chemicals used were of analytical grade. The enzyme was prepared in 0.2 M carbonate bicarbonate buffer at pH 8.0 to reach a final concentration of 1 mg·mL^{-1}. The enzyme solution was divided in plastic tubes of 1 mL and kept in the freezer at −20 °C until the experiments were performed.

Heat treatment

Plastic tubes (1 cm diameter) were filled with the ALP solutions (0.1 mL). The thermal treatment experiments were conducted in a thermostatic water bath (Digibath-2 BAD 4, RaypaTrade, Barcelona, Spain). For the fluorescence spectroscopy investigations, heat treatment was performed for 10 min at constant temperatures ranging from 25 to 70 °C. Taking in consideration the low concentration of the protein solutions, the holding time was considered to be long enough to ensure structural rearrangements within the protein molecule. Only irreversible/permanent protein structure alterations were therefore evaluated. When studying the effect of temperature upon ALP activity, the enzyme solutions were heated at temperatures between 50 and 70 °C in steps of 5 °C for

different holding times (0 to 40 min). No lower temperatures were considered due to enzyme capacity of being stable at temperature below 50 °C. After heating, the tubes were immediately cooled in ice water to prevent further thermal denaturation. For fluorescence spectroscopy investigation, before analyses, 30 μL of ALP solutions were introduced in quartz cuvette containing 3 mL of 0.1 M carbonate-bicarbonate buffer at pH 8.0 and allowed to stand at room temperature for 15 min.

Molecular modeling

The 3D model of ALP molecule was obtained from the Brookhaven Protein Data Bank. The crystal structure of human phosphatase (1EW2.pdb, Le Du et al. 2001) was used in the present study as no information regarding the 3D model of bovine ALP is available in the database. The ALP model was chosen based on the high value of the sequence identities, after performing sequence alignment checks with BLASTN 2.2.29+ Program (Zhang et al. 2000).

The molecular mechanics (energy minimizations) and molecular dynamics (MD) simulations were performed using Gromacs software (Berendsen et al. 1995) in parallelization conditions, on a Intel(R) Core(TM)2 CPU 6300 1.86 GHz processor-based machine running Linux, with the Gromos96 43a1 force field.

After refinement, the ALP model was minimized first in vacuum and afterwards in aqueous environment, using Steepest Descent algorithm. A total of 29,869 single point charge explicit water molecules were used to solvate the ALP model and the system was further heated for 100 ps to different temperatures (25, 50, 60, and 70 °C) during individual molecular dynamics (MD) steps, by means of a Berendsen thermostat. After equilibration for 1 ns, structural particularities of ALP model at different temperatures were checked by means of PDBsum tool (Laskowski 2009). The time step used in all MD simulations was 0.001 ps. The electrostatic interactions were resolved with the Particle-Mesh-Ewald (PME) method with a Coulomb cutoff of 1.7 nm, Fourier spacing of 0.12 nm and a fourth order interpolation. Lennard-Jones potential and switch function with a cutoff distance of 1.1 nm and a switching distance of 0.9 nm were used for treating the van der Waals' interactions.

Fluorescence spectroscopy experiments

The fluorescence spectra of protein were obtained using LS-55 luminescence spectrometer (PerkinElmer Life Sciences, Shelton, CT, USA) equipped with a quartz cell of 10 mm path length. Each spectrum represents the average of three scans. The fluorescence properties of tryptophan (Trp) (phase diagram, fluorescence spectrum, ANS fluorescence and quenching experiments) were performed as described by

Stănciuc et al. (2012). For tyrosine (Tyr) fluorescence the experiments were similar with those described for Trp with the exception that the excitation wavelength was set at 274 nm.

The synchronous fluorescence spectra of ALP were obtained by setting the excitation and emission wavelength interval ($\Delta\lambda$) to be 15 and 60 nm respectively, and scanning within the wavelength range from 250 to 340 nm.

The 3D fluorescence spectra were performed under the following conditions: the emission wavelength was recorded between 200 and 550 nm and the initial excitation wavelength was set at 200 nm with an increment of 10 nm up to 500 nm. Other scanning parameters were identical to those of fluorescence spectra described by Stănciuc et al. (2012).

Enzyme activity

The ALP activity was measured spectrophotometrically at 405 nm, using a UV–VIS GBC Cintra spectrophotometer (GBC Scientific Equipment Pty Ltd, Melbourne, Australia) according to Aschaffenburg and Mullen test (Rankin et al. 2010). ALP solution (50 μL) was added to 2.5 mL of *p*-nitrophenyl phosphate which in reaction with ALP develops a yellow color, an indicator of the liberated nitrophenol. One unit of enzyme activity (U) was estimated as the amount of *p*-nitrophenol, in micrograms, liberated per min at 20 °C. All the experiments were performed at least in triplicate and the errors were lower than 2 %.

Kinetic data analysis

ALP inactivation was described by the first order kinetic model. The kinetic parameter values for thermal inactivation were estimated by linear regression analysis. The temperature dependence of the inactivation rate constants was estimated using the Arrhenius model, as described by Dumitraşcu et al. (2013). All standard deviations and linear regression errors were calculated using Microsoft Excel.

Results and discussion

Investigations at single molecule level

Previous studies showed that, in addition to experiments, MD simulations are important tools for getting new insights into protein structure and function. Fundamental appreciation of biomolecules behavior often requires the conjunction of *in silico* and experimental approaches such as to allow better exploring structural and functional landscape.

MD simulations were used in the present study to gather information at single molecule level on ALP behavior at thermal treatment. The solvated protein was heated at different temperatures ranging from 25 to 70 °C and structural features and energetic descriptors were collected and averaged from the last 100 ps of the equilibration step. Analyzing the results presented in Table 1 one can observe slight changes in helical and strands content with the temperature increase.

The number of helices decreased from 19 to 18 by increasing the temperature from 25 to 60 °C, causing a significant reduction of the helical interacting residues which suggests protein unfolding. Accordingly the total number of beta turns motifs, which are defined by 4 consecutive residues with Cα atoms of the first and last residues at less than 7 Å and having non-helical central residues (Lewis et al. 1973), increased from 54 to 59. Further increase of the temperature to 70 °C generated additional ALP structural rearrangements, favoring the increase of the alpha and 3–10 helical contents up to 29.2 and 3.1 %, respectively, and the decrease of the total number of beta turn motifs to 45.

The change in protein conformation is correlated with molecular features such as volume or solvent-accessible surface. The temperature increase up to 60 °C favored the protein unfolding, reflected in the slight increase of the ALP volume (Table 1); further temperature increase caused volume reduction and therefore protein folding. Based on the temperature dependent evolution of the hydrophobic surface available to the solvent (HSAS) one can presume a different pattern of ALP folding with respect to the native structure (Table 1). As a consequence of local rearrangements with the temperature, new amino acids are exposed to the explicit water molecules, explaining the HSAS increase even when the protein volume decreases. HSAS was calculated through the *in silico* approach and represents ~56.76 % of the total solvent-accessible surface of the ALP at room temperature, and ~56.66 % at 70 °C.

The most important thermally induced conformational changes or transitions of proteins are largely driven by the hydrogen bonding which play a dominant role in protein folding (Dill 1990). The heat treatment caused a slight reduction of the total number of hydrogen bonds (Hb) within ALP structure, but did not affected significantly the Hbs between protein and water molecules (Table 1). The rather good structural stability of ALP against temperature might be partially due to the two disulfide bridges (Cys[121]–Cys[183] and Cys[467]–Cys[474]) which are well conserved among mammalians (Le Du et al. 2001).

The detailed checking of the ALP catalytic site showed that, although there are no significant changes in the overall secondary and tertiary structures of the enzyme with the temperature increase, the involvement of the catalytic residues, Ser[92] and Arg[166], to different secondary structure motifs varies with the temperature. At room temperature both catalytic residues belong to beta-turn motifs, while at temperatures over 60 °C, Ser[92] is the first residue of a 8 amino acids-long helix, interacting with two other helices (Ala[154]–Gly[157] and Thr[456]–

Table 1 Molecular details on ALP under thermal treatment

Descriptors	Temperature			
	25 °C	50 °C	60 °C	70 °C
Structural indicators				
Strands (%)	12.3	16.3	13.8	14
Alpha helix (%)	28.2	27.8	27.6	29.2
3–10 helix (%)	1.9	2.5	2.5	3.1
Helix-helix interactions	13	12	9	13
Sheets	2	3	3	2
Beta alpha beta units	3	3	2	3
Beta hairpin	1	1	1	1
Beta bulge	2	2	3	2
Beta turns	54	53	59	45
Gamma turns	12	12	12	11
Molecular and energetic descriptors				
HBs within the protein	374±9	354±9	360±9	350±7
HBs between protein and water	708±16	717±16	707±14	702±14
Volume, nm^3	75.98±1.69	76.17±1.82	76.58±1.63	75.48±1.36
Total surface	202.65±2.09	204.64±2.23	210.81±2.58	214.91±2.30
Hydrophobic surface, nm^2	115.03±1.31	113.85±1.55	118.55±1.67	121.76±1.47
Potential energy, kJ/mol	$-1.30\cdot10^6\pm873.10$	$-1.26\cdot10^6\pm828.20$	$-1.24\cdot10^6\pm969.55$	$-1.23\cdot10^6\pm966.11$

Ala[465]) and Arg[166] belongs to an unordered secondary structure region.

The alteration of the catalytic site at high temperatures is also indicated by the changes in the hydrogen bonding pattern. At room temperature the catalytic Ser residue is involved in a double Hb with His[358], whereas the side chain of Arg[166] establish contact with the side chain of Tyr[169]. When the temperature was increased up to 60 °C, one of the Hbs responsible for the side chain orientation of Ser[92] disappeared, indicating loosening of the catalytic site, and the new conformation is reinforced at even higher thermal treatment (70 °C) through an additional Hb between Ser[92] and Asp[42]. On the other hand, due to the important rearrangements within the Arg[166] microenvironment, new Hbs involving both the side chain and backbone of catalytic arginine residue are established with Asp[91] and Gln[108], respectively at 60 °C. The conformation of the active site becomes even more rigid at 70 °C because of the double Hb between the side chains of Arg[166] and Gln[108] coupled with the close interaction with Asn[165].

Phase diagram

Investigation of the chemical and biological reactions using fluorescence spectroscopy represents a useful tool in understanding the denaturation mechanisms of protein (Liu et al. 2011). The *phase diagram* method provides detailed information on protein unfolding pathway, allowing identifying eventual partially folded species and intermediates (Kuznetsova

et al. 2004). The linear dependences of I_{365} versus I_{320} indicate the presence of only two different conformations, without any intermediates between native and unfolding states. Therefore, the changes of protein tertiary structure lead to the two state transitions (*all or none transition*). The non-linearity of this function reflects the sequential character of structural transformations.

The dependence of I_{365} by I_{320} was used in this study to detect the existence of any intermediate states of ALP as a function of temperature. Figure 1 shows a linear *phase diagram* that indicates the presence of two structurally distinct
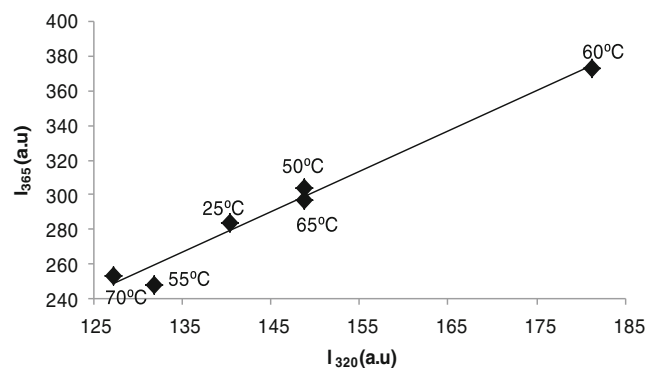

Fig. 1 Phase diagram analysis of heat-induced conformational changes of ALP based on intrinsic fluorescence intensity values measured at wavelengths 320 and 365 nm. The temperature values are indicated in the vicinity of the corresponding symbol. Three independent tests were carried out in each case and SD was lower than 2.5 %

species of ALP induced by temperature increase from 25 to 70 °C.

Analyzing the results presented in Fig. 1 one can conclude that, the dissociation of the ALP dimers followed by the unfolding of the native state predominates up to 60 °C, causing the exposure of the hydrophobic residues, accompanied by a sequential increase of fluorescence intensity. The decrease in fluorescence intensity at temperatures higher than 60 °C is due to folding of protein molecules. These results are in agreement with the *in silico* observations at single molecule level.

Fluorescence intensity

The intrinsic fluorescence of proteins is generated by Trp, Tyr, and phenylalanine (Phe) residues, out of which Trp fluorescence intensity is stronger upon excitation wavelength higher than 280 nm. Trp and Tyr residues were used to follow protein structural alterations, knowing the dependence of their fluorescence properties on the environment changes which involves protein folding/unfolding (Royer 2006). In the native folded state, Trp residues are generally located within the core of the protein, whereas in a partially folded or unfolded state, they become exposed to solvent. According to Mersol et al. (1991) each monomer ALP molecule has three Trp residues located in positions 109, 220 and 268, out of which only Trp[109] is exposed and phosphoresces at room temperature.

For the whole tested range, the increase of temperature resulted in the decrease of fluorescence intensity (Fig. 2). In the selected temperature range of 25–60 °C, the ALP solutions excited at 295 nm exhibited a broad emission band centered at 345–347 nm (Fig. 2a), whereas at higher temperature a red-shift of 5 nm was observed when compared with untreated protein solutions.

The λ_{max} of buried Trp residues is around 335 nm, whereas Trp residues fully accessible to the solvent have λ_{max} around 355 nm. Therefore, the Trp residues of ALP are partially exposed up to 60 °C and totally exposed to solvent at higher temperature. However, given the results presented in *phase diagram* and MD experiments, we presume that at higher temperature, ALP polypeptide chains fold following a different pattern compared the initial state of protein, which leads to higher exposure of Trp residues.

Usually, the emission maximum of Tyr residues is about 305 nm and is not influenced by the polarity of the environment (Gonzalez-Horta et al. 2013). In our study, the emission spectra shows an emission band for Tyr with maximum at 345 nm at 25 °C, followed by a small blue-shift of 1–2 nm up to 55 °C (Fig. 2b). A red-shift of 5 nm was recorded when heating the protein at 65 °C, followed by a blue-shift of 5 nm at 70 °C, suggesting that the environment of Tyr residues is changing from a hydrophobic to a more hydrophilic at higher temperature. Anyway, Tyr emission was shown to depend on pH (Gonzalez-Horta et al. 2013). At high pH values the
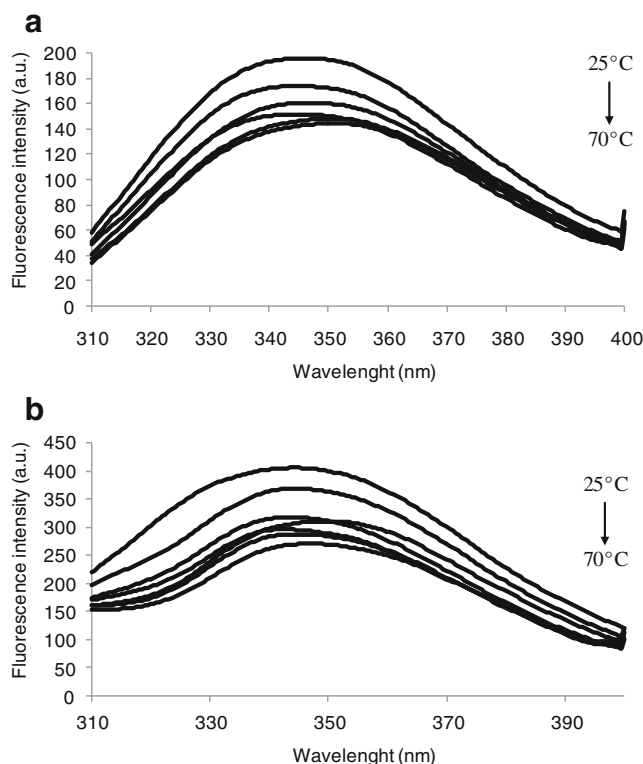
Fig. 2 Structural changes of ALP monitored by emission spectrum. The excitation wavelengths were 292 nm (**a**) and 274 nm (**b**). Three independent tests were carried out in each case and SD was lower than 3.5 %

phenolic hydroxyl group, which has a pKa near 10, is deprotonated, causing the formation of tyrosinate, which gives a red-shift in the emission spectrum (Munishkina and Fink 2007).

Synchronous spectrum

The use of synchronous fluorescence spectroscopy technique provides several advantages, such as sensitivity, spectral simplification, spectral bandwidth reduction and avoiding different perturbing effects (Ashoka et al. 2006). This method is a very useful tool to study proteins behavior based on the microenvironment of amino acid residues, by measuring the shifts of the emission wavelength. As it has been mentioned previously, ALP possesses intrinsic fluorescence arising from Trp, Tyr and Phe residues. The particularities of Tyr and Trp residues in different environmental conditions can be investigated by setting the excitation and emission wavelength interval ($\Delta\lambda$) to 15 and 60 nm, respectively (Ehteshami et al. 2013). The effects of heating on ALP synchronous fluorescence spectra are shown in Fig. 3.

From Fig. 3a, it can be observed that λ_{max} remains constant at 286 nm in the temperature range of 25 to 60 °C, with a small blue-shift of 2 nm at higher temperatures. The fluorescence of Trp residues remains also constant at 278 nm (Fig. 3b). These
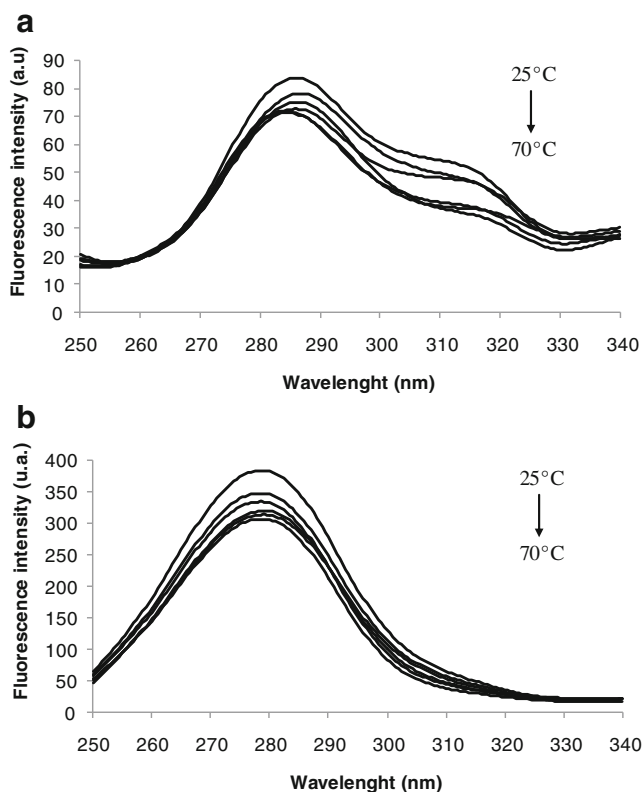
Fig. 3 Synchronous fluorescence spectra of ALP at different temperature: **a** $\Delta\lambda=15$ nm and (**b**): $\Delta\lambda=60$ nm. Three independent tests were carried out in each case and SD was lower than 3.0 %

results suggested that, regardless of the temperature values, the polarity around both Trp and Tyr residues is rather preserved.

Three-dimensional fluorescence spectroscopic studies

The technology based on three-dimensional fluorescence spectra has been proved to be a powerful analytical tool that can provide complete description on proteins fluorescence. The representative three-dimensional fluorescence spectra and map contours of ALP treated at different temperatures are shown in Fig. 4.

For all thermally treated ALP samples two fluorescence peaks were recorded. The location of peaks 1 and 2 for the ALP samples at 25 °C is given by $\lambda_{ex}/\lambda_{em}$ of 280 nm/348 nm and 220 nm/342 nm respectively. In addition, two Rayleigh scattering peaks (peak A and B) could be easily observed in the isometric three-dimensional projection or the three-dimensional fluorescence contour map of ALP. Regardless of the temperature, the contour map displayed a bird's eye view of the fluorescence spectra. As the protein was excited at 280 nm, mainly information on the intrinsic fluorescence of Trp and Tyr residues was collected (Liu et al. 2011). Therefore, peak 1 reveals the spectral characteristic of Trp and Tyr residues. Heat treatment up to 60 °C resulted in a 3–5 nm blue shift in peak 1, indicating changes in the polarity of

the hydrophobic microenvironment of Trp and Tyr residues of ALP. At higher temperatures, a 4–5 nm red-shift of peak 1 indicates a more advanced exposure of hydrophobic residues to the solvent. The fluorescence intensity decreased in the whole tested temperature range, with a maximum of 25 % at 65 °C.

Peak 2 mainly reveals the spectral behavior of polypeptide backbone, and its fluorescence intensity is related to the protein secondary structure (Paul and Guchhait 2011). When compared to the protein solutions tempered at room temperature, a blue-shift of 3 nm was recorded at temperatures up to 65 °C, followed by a red-shift of 2 nm at 70 °C. The intensity of peak 2 decreased in the whole temperature range, the most important decrease of 50 % being noticed at 50 °C.

Taking into account the above mentioned phenomena as well as the findings on the fluorescence characteristics of the peaks one can conclude that the heat-treatment caused a sequential different pattern of unfolding and refolding of polypeptide chains which involve an advanced Trp exposure to the solvent.

Quenching experiments

Fluorescence after excitation at 292 nm is mainly contributed by the Trp residue alone. When small molecules interact with proteins, this fluorescence may be quenched. In order to further probe the heat induced changes in Trp microenvironment and their exposure to solvent during (un-)folding, fluorescence quenching experiments using acrylamide and KI were performed. The acrylamide quenching process is very efficient as all Trp residues are accessible to the quencher. On the other hand, ionic quenchers like KI, which have charged and strongly hydrated character, can quench only the fluorescence emitted by fully exposed Trp residues.

The data for the acrylamide and KI quenching of ALP were calculated by using Stern-Volmer equation. When performing quenching experiment with acrylamide, the highest and lowest quenching constant (K_{sv}) values were obtained for the untreated protein solutions (4.05 ± 0.86 mol^{-1} L), and respectively for the protein solutions heat-treated at 55 °C (2.32 ± 0.55 mol^{-1} L) (Table 2). When performing quenching with KI, no significant differences were observed for the K_{sv} values (Table 2).

As expected, the quenching constants calculated for experiments with acrylamide are significantly higher with respect to KI. When compared to K_{SV} value for free Trp of 22.0 ± 0.5 mol^{-1} L (Chadborn et al. 1999), it is obvious that Trp residues from ALP molecule show lower accessibility to the quencher. Regardless of temperature, part of the residues is exposed, while some other residues are buried within the protein matrix. The decrease of the quenching constants in the whole temperature range (Table 2) indicates
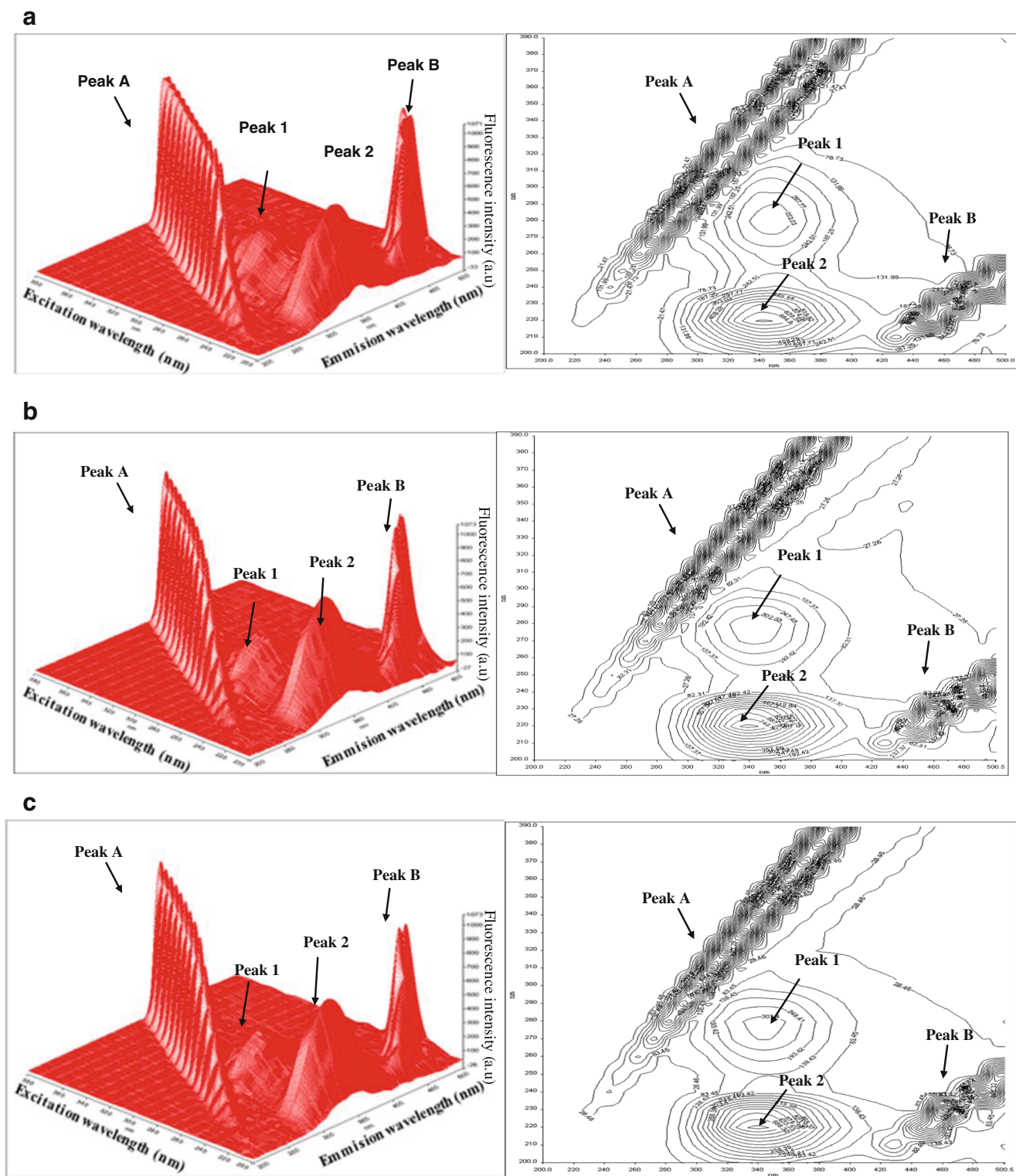
Fig. 4 The three-dimensional fluorescence projections and three-dimensional fluorescence contour map of ALP at 25 °C (**a**), 50 °C (**b**), 55 °C (**c**), 60 °C (**d**), 65 °C (**e**) and 70 °C (**f**)

conformational transitions of ALP with local structural rearrangements and partial additional burial of Trp residues leading to the decrease of the distance between the Trp residues and quenchers.
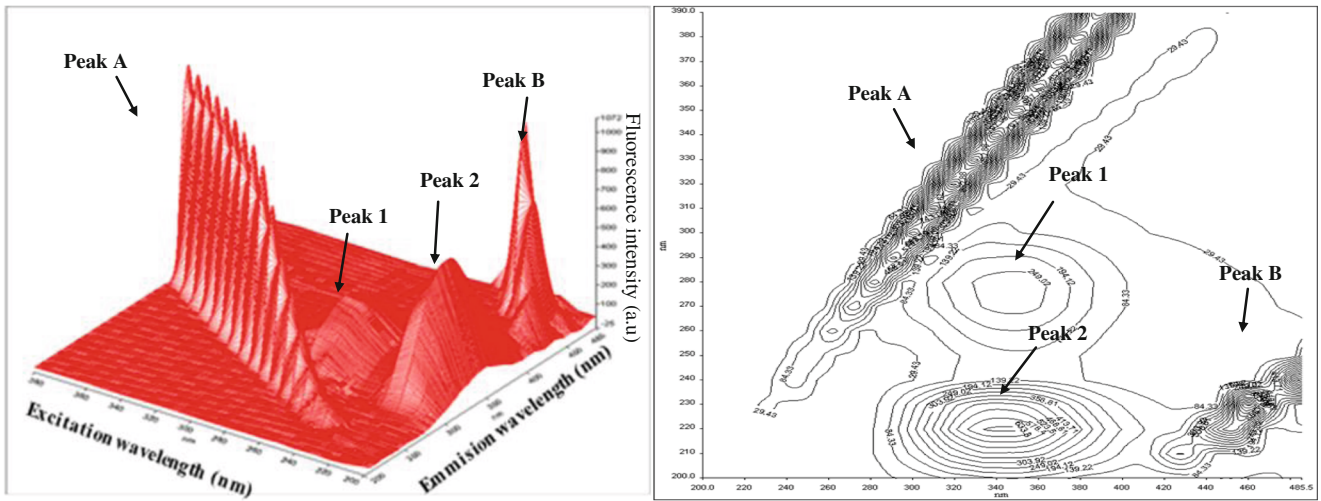
ANS fluorescence intensity

ANS is a non-covalent extrinsic fluorescent probes commonly used for studying protein folding. Because of this, ANS is

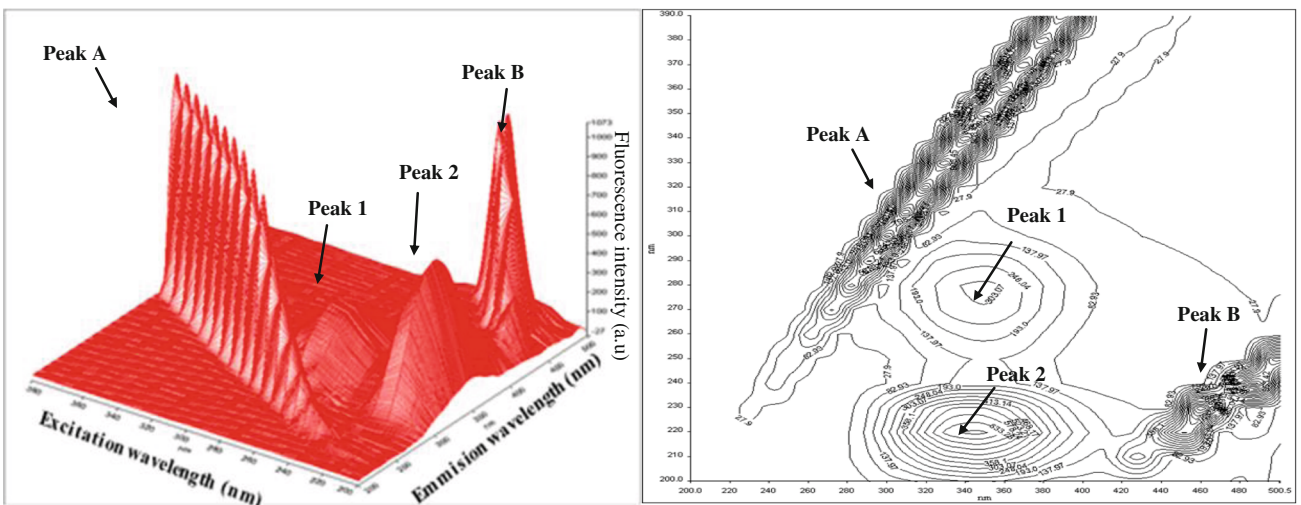**d**
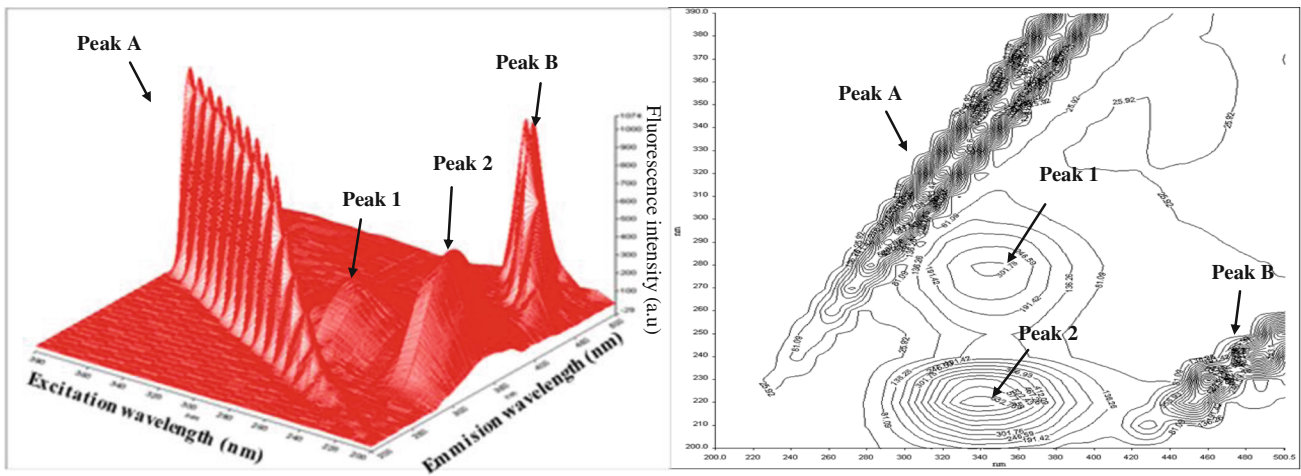
e

f

Fig. 4 (continued)

Table 2 Stern–Volmer quenching constants (mol^{-1} L) and rate constant (min^{-1}) of thermal denaturation ALP solutions

Temperature (°C)	Acrylamide		KI		k×10^{-2}
	K_{SV}	R^b	K_{SV}	R	
25	4.05±0.63^a	0.99	1.54±0.45	0.99	nd
50	2.49±0.50	0.97	1.99±0.33	0.98	6.37±0.52
55	2.32±0.70	0.99	0.85±0.20	0.98	17.41±0.58
60	2.83±0.35	0.99	1.23±0.65	0.99	52.25±1.36
65	2.79±0.72	0.99	1.73±0.42	0.99	182.42±16.08
70	2.89±0.82	0.99	1.75±0.32	0.99	548.39±27.71

nd not determined

^{a} Standard errors

^{b} Correlation coefficient values

widely used to detect and characterize protein-folding intermediates. The fluorescence intensity of ANS increases when the dye binds to the hydrophobic regions of a protein and the intensity maximum of the fluorescence emission is shifted from 510 nm, corresponding to free ANS, to a broad maximum at 470 nm, corresponding to the ANS-protein complex. At 25 °C, λ_{max} was 522 nm, whereas the heat treatment at 50 °C caused a blue-shift to 520 nm, followed by a 3 nm red-shift at 60 °C, indicating that previously buried hydrophobic regions of the protein are exposed. In agreement with previous fluorescence based experiments, the ANS fluorescence intensity measurements indicate ALP folding at higher temperatures, along by burial of the hydrophobic regions: λ_{max} was 522 at 65 °C and 520 nm at 70 °C. There were no significant changes in fluorescence intensity with increasing temperature.

Thermal inactivation

The decrease of ALP activity in buffer solution after heating at different temperatures for 5 min is depicted in Fig. 5.

After 5 min of heating at 50 °C, the ALP activity decreased to 87.69±4.40 %, whereas when heating up to 55 °C only 50 % of the enzyme activity was preserved. Therefore, as
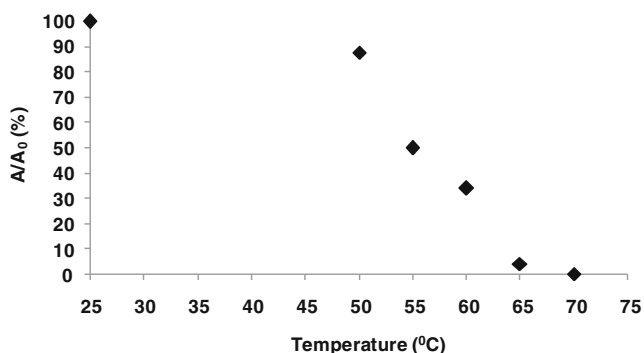
the heat treatment was more severe, the enzyme inactivation was more advanced. The kinetic parameters estimation for ALP inactivation was obtained as described by Claeys et al. (2002), Castro et al. (2004), Marchand et al. (2009). At each temperature, the kinetics of ALP inactivation followed a first order kinetic model (Fig. 6).

Using the linear regression analysis, the inactivation rate constant (k) for ALP at different temperatures was calculated from the slope of ln (A/Ao) versus time. The k values are summarized in Table 2.

The results show that ALP is more stable when treated at low temperatures. When the ALP solutions were heated to 55 °C, the k value was 17.41±0.58 min-1, whereas the temperature increase up to 70 °C led to k value 90 times higher compared to 50 °C. Fadiloĝlu et al. (2005) studied the thermal inactivation of ALP in glycine buffer, raw milk and pasteurized milk. Concerning the ALP activity in buffer heated at 50, 60, 70 and 80 °C, the authors reported k values of 3.90, 6.26, 18.28 and 76.77 min^{-1} respectively, which are rather low compared to our results. According to Arrhenius equation, activation energy (E_a) was calculated by plotting the natural logarithm of the rate constant against the reciprocal of the absolute temperature in Kelvin (T). For the temperature range studied an E_a value of 207.26±21.68 (kJ mol^{-1}) was calculated, which is higher compared to the value reported by Fadiloĝlu et al. (2005) for ALP from calf intestine in glycine buffer (E_a value of 97.2 kJmol^{-1}) or by Stănciuc et al. (2011) (E_a value of 152.05±7.67 kJ mol^{-1}). These differences in terms of k and E_a values between our results and literature might be attributed to the different conditions applied in performing the study, like concentration of ALP enzyme solution used for analysis, and different methods used for quantifying ALP activity.

Having in consideration the importance of ALP for dairy industry, E_a values were also compared with those reported for ALP inactivation in different species of milk. In cow milk E_a values varied from 106.4 to 432.6 kJ·mol^{-1} (Stănciuc et al. 2011; Fadiloĝlu et al. 2005; Wilinska et al. 2007; Claeys et al.
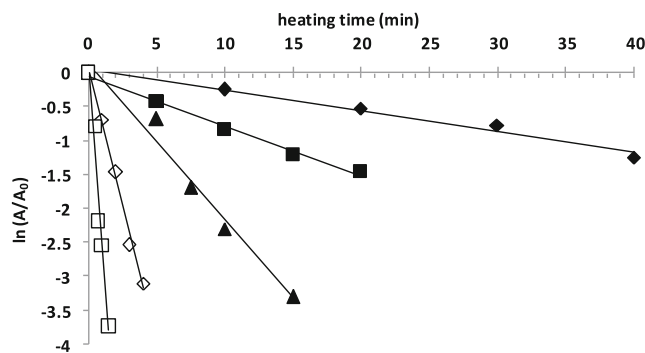

Fig. 5 Thermal stability of ALP at various temperatures after 5 min of holding

Fig. 6 Thermal inactivation of ALP at different temperatures: *black diamond* 50 °C, *black square* 55 °C, *black triangle* 60 °C, *white diamond* 65 °C, *white square* 70 °C. A is the enzyme activity concentration at time t, A_o the initial enzyme activity

2002; Dumitraşcu 2012), for goat milk between 373.04 and 406 373.04 kJ·mol^{-1} (Wilinska et al. 2007; Dumitraşcu 2012), whereas for sheep milk Dumitraşcu (2012) reported an E_a value of 378.52±1.45 kJ·mol^{-1}. Regardless of milk origin, all the studies conducted revealed that ALP is more temperature resistant in milk, the complex matrix of milk providing a protective effect on ALP.

Conclusions

The fluorescence spectroscopy and molecular modeling techniques were used to investigate the thermal dependent behavior of alkaline phosphatase. The emissive properties, structural motifs and kinetic parameters of alkaline phosphatase, obtained in the temperature range of 25 to 70 °C were compared.

The fluorescence spectroscopy results revealed that alkaline phosphatase thermal denaturation involved a complex mechanism that was attributed to sequential unfolding between 25 and 60 °C, followed by folding of polypeptide chains at higher temperatures. Additional key insights on alkaline phosphatase structure were obtained after performing MD simulations. The thermal treatment favored the hydrophobic exposure and important alteration of the catalytic site was observed at temperature over 60 °C. The results were correlated with enzyme activity in buffer solutions. The inactivation studies showed that alkaline phosphatase is more thermoresistant at lower temperatures. Therefore, after 5 min of heating at 50 °C, the enzyme relative activity decreases with 12.31 %. The kinetic data for the analyzed temperature range were fitted using the first order kinetic model and provided a good description of thermal inactivation of the studied enzyme.

The knowledge of structural and catalytic features at thermal treatment provides the molecular basis for better design of further alkaline phosphatase applications.

References

Ashoka S, Seetharamappa J, Kandagal PB, Shaikh SMT (2006) Investigation of the interaction between trazodone hydrochloride and bovine serum albumin. J Lumin 121:179–186

Berendsen HJC, van der Spoel D, van Drunen R (1995) GROMACS: a message-passing parallel molecular dynamics implementation. Comput Phys Commun 91:43–56

Castro I, Macedo B, Teixeira JA, Vicente AA (2004) The effect of electric field on important food-processing enzymes: comparison of inactivation kinetics under conventional and ohmic heating. J Food Sci 69:696–701

Chadborn N, Bryant J, Bain AJ, O'Shea P (1999) Ligand-dependent conformational equilibria of serum albumin revealed by tryptophan fluorescence quenching. Biophys J 76:2198–2207

Claeys W, van Loey A, Hendricks M (2002) Kinetics of alkaline phosphatase and lactoperoxidase inactivation, and of β-lactoglobulin denaturation in milk with different fat content. J Dairy Res 69:541–553

Dill KA (1990) Dominant forces in protein folding. Biochemistry 29(31): 7133–7155

Dumitraşcu, L (2012) Intrinsic indicators for evaluation of heat treatment applied in dairy industry. PhD Thesis, University Dunărea de Jos of Galati, Galati, România

Dumitraşcu L, Moschopoulou E, Aprodu I, Stanciu S, Râpeanu G, Stănciuc N (2013) Assessing the heat induced changes in major cow and non-cow whey proteins conformation on kinetic and thermodynamic basis. Small Rumin Res 111:129–138

Ehteshami M, Rasoulzadeh F, Mahboob S, Rashidi MR (2013) Characterization of 6-mercaptopurine binding to bovine serum albumin and its displacement from the binding sites by quercetin and ruti. J Lumin 135:164–169

Fadiloğlu S, Erkmen O, Şekeroğlu G (2005) Thermal inactivation kinetics of alkaline phosphatase in buffer and milk. J Food Process Pres 30(3):258–268

Fox PF, Kelly AL (2006) Indigenous enzymes in milk: overview and historical aspects—Part 2. Int Dairy J 16:517–532

Gonzalez-Horta A, Gonzalez Hernandez B, Chavez-Montes A (2013) Fluorescence as a tool to study lipid-protein interactions: the case of α-synuclein. Open J Biophys 3:112–119

Hung HC, Chang GG (2001) Multiple unfolding intermediates of human placental alkaline phosphatase in equilibrium urea denaturation. Biophys J 81:3456–3471

Knight AH, Fryer SM (1989) The development of heat-resistant phosphatase activity in raw milk. Int J Dairy Technol 42:81–86

Kuznetsova M, Turoverov KK, Uversky VN (2004) Use of the phase diagram method to analyze the protein unfolding-refolding reactions: fishing out the "invisible" intermediates. J Proteome Res 3: 485–494

Laskowski RA (2009) PDB sum new things. Nucleic Acids Res 37: D355–D359

Le Du MH, Stigbrand T, Taussig MJ, Menez A, Stura EA (2001) Crystal structure of alkaline phosphatase from human placenta at 1.8 Å resolution. Implication for a substrate specificity. J Biol Chem 276(12):9158–9165

Lewis PN, Momany FA, Scheraga HA (1973) Chain reversals in proteins. Biochim Biophys Acta 303:211–229

Liu J, Campos LA, Cerminara M, Wang X, Ramanathan R, English DS, Muñoz V (2011) Exploring one-state downhill protein folding in single molecules. Proc Natl Acad Sci U S A 109:179–184

Liu S, Pang S, Na W, Su X (2014) Near-infrared fluorescence probe for the determination of alkaline phosphatase. Biosens Bioelectron 55: 249–254

Marchand S, Merchiers M, Messens W, Coudijzer K, De Block J (2009) Thermal inactivation kinetics of alkaline phosphatase in equine milk. Int Dairy J 19:763–767

Mersol JV, Steel DG, Gafni A (1991) Quenching of tryptophan phosphorescence in *Escherichia coli* alkaline phosphatase by long-range transfer mechanisms to external agents in the rapid-diffusion limit. Biochemistry 30:668–675

Michio S, Satoshi K, Tohru Y, Koreaki I (1997) Roles of disulfide bond in bacterial alkaline phosphatase. J Biol Chem 272:6174–6178

Munishkina LA, Fink LA (2007) Fluorescence as a method to reveal structures and membrane-interactions of amyloidogenic proteins. Biochim Biophys Acta 1768:1862–1885

Paul BK, Guchhait N (2011) A spectral deciphering of the binding interaction of an intramolecular charge transfer fluorescence probe with a

cationic protein: thermodynamic analysis of the binding phenomenon combined with blind docking study. Photochem Photobiol Sci 10:980–991

Rankin SA, Christiansen A, Lee W, Banavara DS, Lopez-Hernandez A (2010) The application of alkaline phosphatase assays for the validation of milk product pasteurization. J Dairy Sci 93: 5538–5551

Royer AC (2006) Probing protein folding and conformational transitions with fluorescence. Chem Rev 106:1769–1784

Stănciuc N, Ardelean AI, Diaconu V, Râpeanu G, Stanciu S, Nicolau A (2011) Kinetic and thermodynamic parameters of alkaline phosphatase and γ–glutamyl transferase inactivation in bovine milk. Dairy Sci Technol 91:701–717

Stănciuc N, Aprodu I, Râpeanu G, Bahrim G (2012) Fluorescence spectroscopy and molecular modeling investigations on the thermally induced structural changes of bovine β-lactoglobulin. Innov Food Sci Emerg 15:50–56

Wang JZ, Lee J, Sia YX, Wang W, Yang JM, Yin SJ, Qian GY, Park YD (2014) A folding study of Antarctic krill (Euphausia superba) alkaline phosphatase using denaturants. Int J Biol Macromol 70:266–274

Wilińska A, Bryjak J, Illeová V, Polakovič M (2007) Kinetics of thermal inactivation of alkaline phosphatase in bovine and caprine milk and buffer. Int Dairy J 17:579–586

Zalatan JG, Fenn TD, Herschlag D (2008) Comparative enzymology in the alkaline phosphatase superfamily to determine the catalytic role of an active-site metal ion. J Mol Biol 384:1174–1189

Zhang Z, Schwartz S, Wagner L, Miller W (2000) A greedy algorithm for aligning DNA sequences. J Comput Biol 7(1–2):203–214